



Repositorio Institucional de la Universidad Autónoma de Madrid

<https://repositorio.uam.es>

Información suplementaria del artículo publicado en:

This is the **electronic supporting information** (ESI) author version of a paper

published in:

ACS Catalysis 7.2 (2017): 1015-1024

DOI: <https://doi.org/10.1021/acscatal.6b03043>

Copyright: © 2016 American Chemical Society

SUPPORTING INFORMATION

An AZA-Fused π -Conjugated Microporous Framework Catalyst for the Production of Hydrogen Peroxide

V. Briega-Martos,[†] A. Ferre-Vilaplana,^{‡,§} A. de la Peña,^{⊥,Σ} J. L. Segura,[⊥] F. Zamora,^{*,Σ} J. M. Feliu,[†] and E. Herrero^{*,†}

[†] *Instituto de Electroquímica, Universidad de Alicante, Apdo 99 E-03080, Alicante, Spain*

[‡] *Instituto Tecnológico de Informática, Ciudad Politécnica de la Innovación, Camino de Vera s/n, E-46022 Valencia, Spain*

[§] *Departamento de Sistemas Informáticos y Computación, Escuela Politécnica Superior de Alcoy, Universidad Politécnica de Valencia, Plaza Ferrándiz y Carbonell s/n, E-03801 Alcoy, Spain*

[⊥] *Departamento de Química Orgánica, Facultad de Química, Universidad Complutense de Madrid, E-28040, Madrid, Spain*

^Σ *Departamento de Química Inorgánica e Instituto de Física de la Materia Condensada (IFIMAC), Facultad de Ciencias. Universidad Autónoma de Madrid, E-28049, Madrid, Spain*

Corresponding Authors

* herrero@ua.es, felix.zamora@uam.es

List of Additional Figures:

Figure S1. Solid state ^{13}C CP/MAS NMR spectrum of **Aza-CM**.

Figure S2. FT-IR Spectra profiles.

Figure S3. Thermo-gravimetric properties of **Aza-CMP**.

Figure S4. X-Ray Powder Diffraction Patterns of **Aza-CM**.

Figure S5. Pore parameters of **Aza-CMP**.

Figure S6. DC Conductivity measurements of **Aza-CMP**.

Figure S7. Exfoliation and AFM of **Aza-CMP**.

Figure S8. Co $2p_{3/2}$ XPS spectra of the **Aza-CMP@Co**

Figure S9. Supercell model of the **Aza-CMP**.

Figure S10. Adsorbent-adsorbate-solvent configuration corresponding to the fully optimized monodentate associative chemisorbed state of an oxygen molecule on top of the **Aza-CMP**.

Materials and Methods

All chemicals and solvents were obtained from Aldrich Chemical Co. and used without further purification. Solvents and reagents for the preparation of these materials were dried by usual methods prior to use and typically used under inert gas atmosphere.

Elemental microanalyses, Thermogravimetric analyses, solid state ^{13}C CP-MAS nuclear magnetic resonance spectroscopy were performed at the Universidad Autónoma de Madrid, Spain, Servicio Interdepartamental de Investigación. IR spectra were recorded at the Organic Chemistry Department of the Universidad Complutense de Madrid.

Solid-State ^{13}C CP-MAS Nuclear Magnetic Resonance Spectroscopy. High Resolution solid-state nuclear magnetic resonance (NMR) spectra were recorded at ambient pressure on a Bruker AV 400 WB spectrometer using a triple channel (BL4 X/Y/ ^1H) and Bruker magic angle-spinning (MAS) probe with 4 mm (outside diameter) zirconia rotors. The magic angle was adjusted by maximizing the number and amplitudes of the signals of the rotational echoes observed in the ^{79}Br MAS FID signal from KBr. Cross-polarization with MAS (CP-MAS) used to acquire ^{13}C data at 100.61 MHz. The ^1H ninety degree pulse widths were both 3.1 μs . The CP contact time varied from 3.5 ms. High power two-pulse phase modulation (TPPM) ^1H decoupling was applied during data acquisition. The decoupling frequency corresponded to 80 kHz. The MAS sample spinning rate was 10 kHz. Recycle delays between scans were 4 s, depending upon the compound as determined by observing no apparent loss in the ^{13}C signal from one scan to the next. The ^{13}C chemical shifts are given relative to tetramethylsilane as zero ppm, calibrated using the methylene carbon signal of adamantane assigned to 29.5 ppm as secondary reference.

FT-IR Spectroscopy. IR spectra were recorded on Shimadzu FTIR 8300 as KBr pellets. Most important signals are reported in cm^{-1} .

Thermogravimetry. Thermogravimetric Analyses of samples were run on a Thermobalance TGA Q-500 thermal gravimetric analyzer with samples held in a platinum pan under nitrogen atmosphere. A 10 K min^{-1} ramp rate was used.

Microanalyses. Elemental microanalyses were obtained using LECO CHNS-932 elemental analyzer.

X-Ray Diffraction measurements. X-Ray diffraction (XRD) patterns were recorded using $\text{CuK}\alpha$ radiation ($\lambda = 1.5406\text{\AA}$) on a Philips PANalytical X' Pert PRO diffractometer operating at 45 kV and 40 mA between 0.7 and 10° (2θ) at a step size of 0.0300° .

Determination of Pore Paramentes. Nitrogen adsorption-desorption isotherms were measured at 77K in a Micromeritics Tristar 3000 sorptometer. Prior to measurements, a degasification step at 150°C during 8h was performed in nitrogen flux. Surface area was calculated by using the B.E.T. equation in the P/P_0 range from 0.05 to 0.20. Pore size distribution was obtained from the adsorption branch of the isotherms by means of the B.J.H. model.

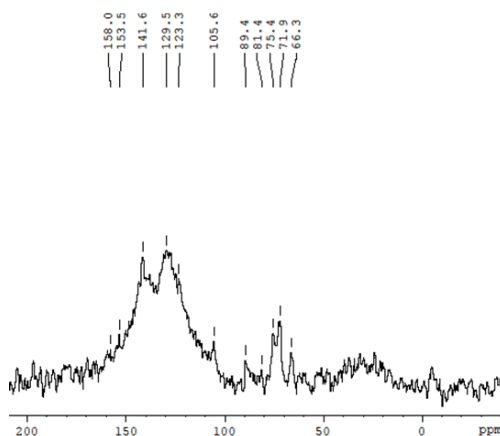
XPS measurements. Spectra on the different samples were collected using a K-Alpha spectrometer of Thermo-Scientific.

AFM Measurements. Atomic Force Microscope (AFM) techniques were used in dynamic mode using a Nanotec Electronica system operating at room temperature in ambient air. conditions. The images were processed using WSxM (freely downloadable scanning probe microscopy software from www.nanotec.es). For AFM measurements, commercial Olympus Si/N and Ti/Pt cantilevers were used with a nominal force constant of 0.75 N/m and 2 N/m, respectively. The surfaces used for AFM experiments were SiO₂ (300 nm thickness)/Si (IMS Company).

Surface preparations. In order to obtain reproducible results, very flat substrates were used with precisely controlled chemical functionalities, freshly prepared just before the chemical deposition. SiO₂ surfaces were sonicated for 15 min in acetone and 15 min in 2-propanol and then dried under an Argon flow.

Figure S1.

A)



B)

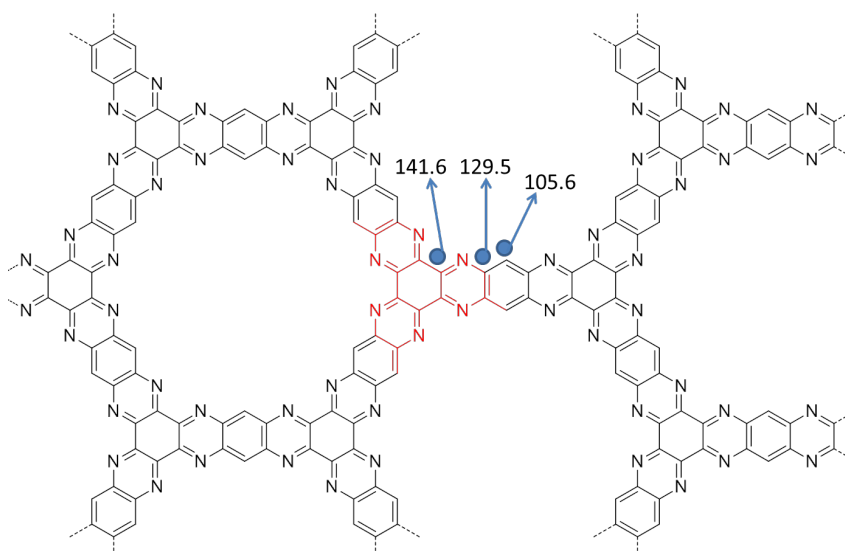


Figure S1. A) Solid state ^{13}C CP/MAS NMR spectrum of **Aza-CMP**. B) Structure of **Aza-CMP** showing the correspondence between the carbon atoms and the signals observed in the NMR spectrum.

In ^{13}C CP/MAS NMR spectra are observed three signals corresponding to the three different carbon atoms in the polymer. The signal at 141 ppm corresponds to the carbon atoms of the phenyl edges connected to aza units, the signal at 129 ppm can be assigned to the carbon atoms of the triphenylene cores on vertices, and the signal at 105 ppm is due to the carbon atoms of the phenyl edges.

Figure S2.

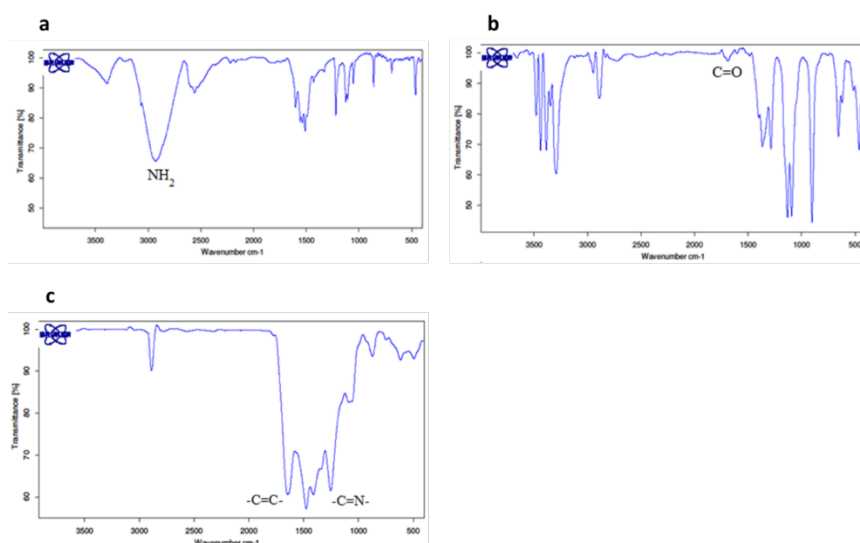


Figure S2. FT-IR Spectra profiles in KBr pellets of *(a) 1,2,4,5-benzenetetramine tetrahydrochloride, (b) hexaketocyclohexane octahydrate and (c) **Aza-CMP**.

In the hexaketocyclohexane octahydrate can be observed a band corresponding to the symmetric tension vibration (**C=O st**) at 1687 cm^{-1} . The 1,2,4,5-benzenetetramine shows the broad band corresponding to the symmetrical stretching vibration (**NH₂ st**) at 2926 cm^{-1} .

For the **Aza-CMP** can be observed the following bands: 2889, 1644, 1477, 1412, 1253, 1087, 872, 745, 616, 495. The band corresponding to the symmetric stretching vibration **C=C st** appears at 1644 cm^{-1} while the signal corresponding to the C-C vibrations of the aza-aromatic rings is located at 1475 cm^{-1} . At 1253 cm^{-1} can be observed the band corresponding to the symmetric tension vibration **C=N st**.

Figure S3.

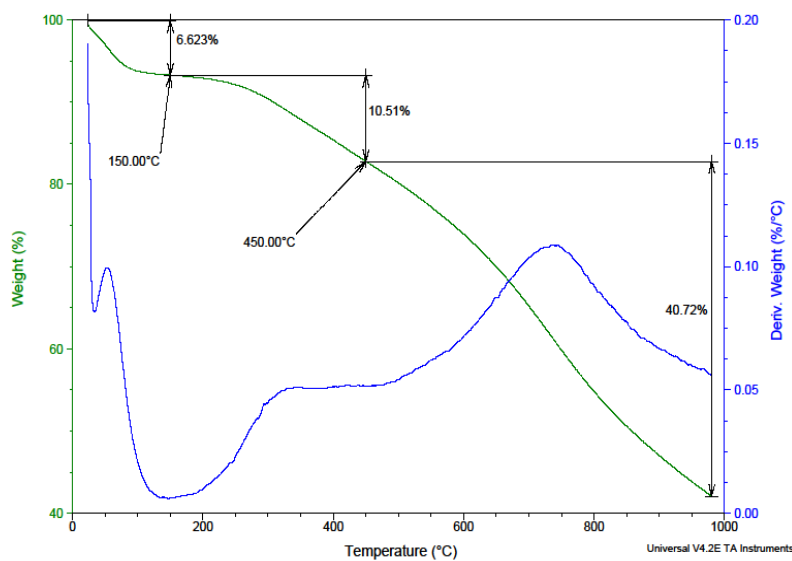


Figure S3. Thermo-gravimetric properties of **Aza-CMP**.

Thermogravimetric analysis (TGA) of **Aza-CMP** shows <10% weight loss at 150 °C probably due to the loss of volatiles (H₂O, DMF) included in the pores and <20% at 450 °C indicating the high thermal stability of **Aza-CMP**.

Figure S4.

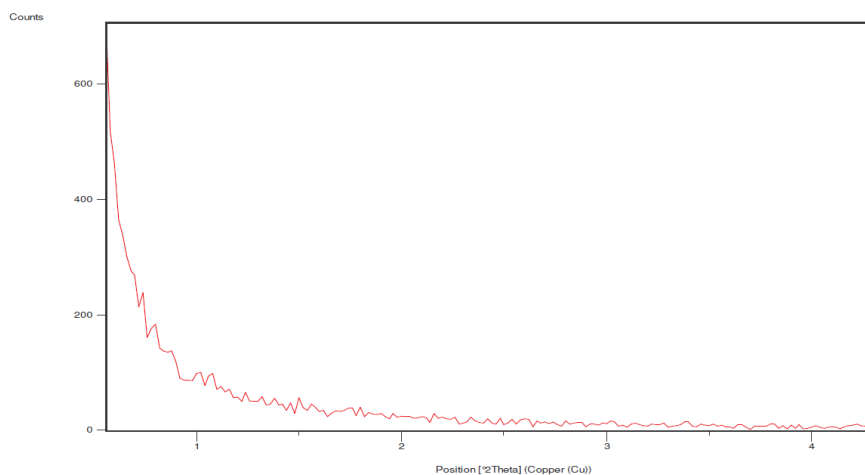


Figure S4. X-Ray Powder Diffraction Patterns of **Aza-CMP**.

Aza-CMP is amorphous and do not show clear peaks in X-ray powder diffraction measurements.

Figure S5.

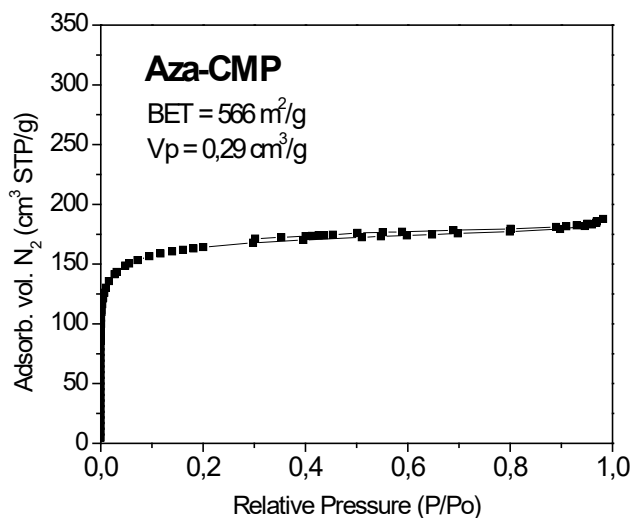


Figure S5. Nitrogen sorption isotherm curve of **Aza-CMP**.

To investigate the porous structure of **Aza-CMP**, nitrogen sorption isotherms were measured at 77 K (Figure S4). It exhibits typical type I isotherms which are characteristic of microporous materials. The Brunauer-Emmet-Teller (BET) surface area and pore volume of **Aza-CMP** were calculated to be 566 m²/g and 0.29 cm³g⁻¹, respectively.

Figure S6.

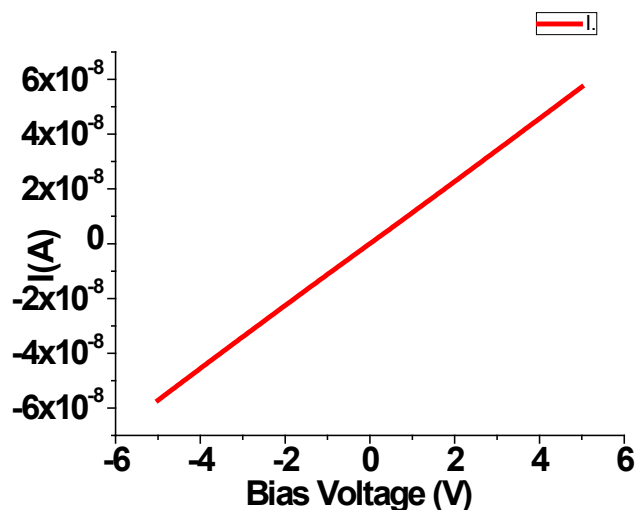


Figure S6. DC Conductivity measurements at 300 K on pressed pellets (6.5 Tons for 5 min.) of **Aza-CMP**. The calculated conductivity value is *ca.* 3×10⁻⁵ Sm⁻¹.

Figure S7.

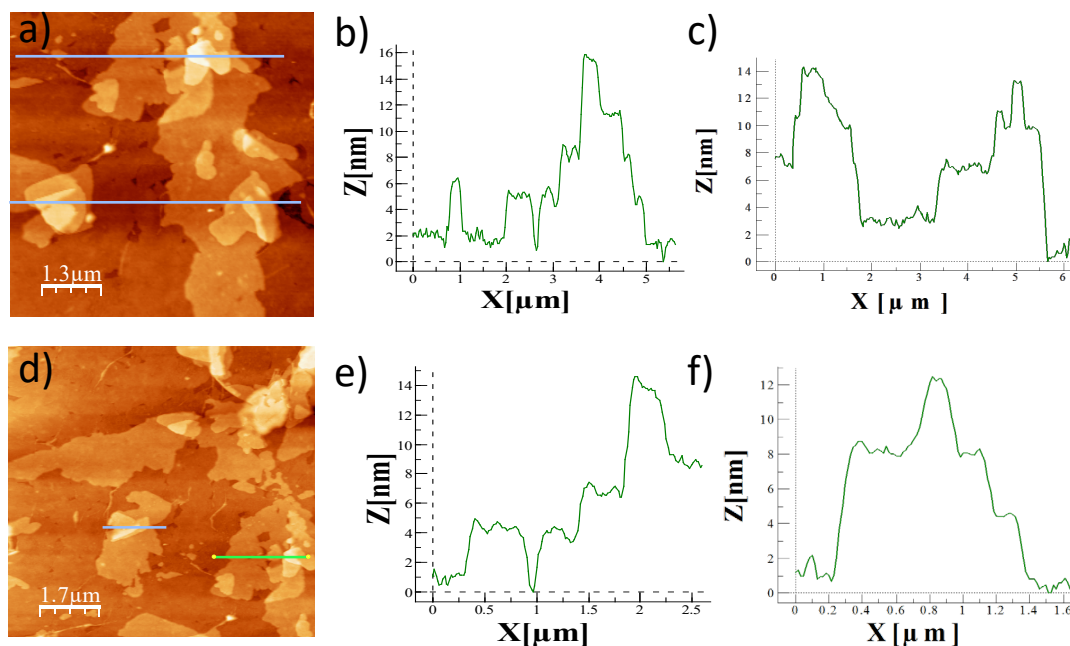


Figure S7. Large areas AFM topographic images (a,d) of a diluted dichloromethane suspension **Aza-CMP** deposited on SiO₂ and their corresponding height profiles along the lines (b,c and e,f, respectively) showing large density of nanolayers with a minimum height of *ca.* 2 nm and over micron length lateral dimensions.

Figure S8.

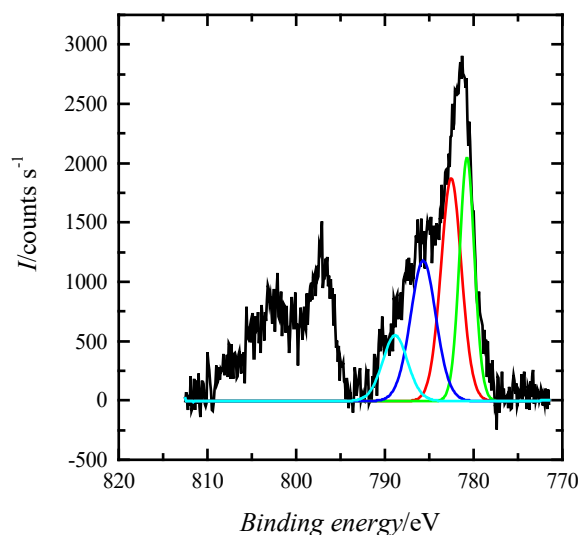


Figure S8. Co 2p_{3/2} XPS spectra of the Aza-CMP@Co

Figure S9.

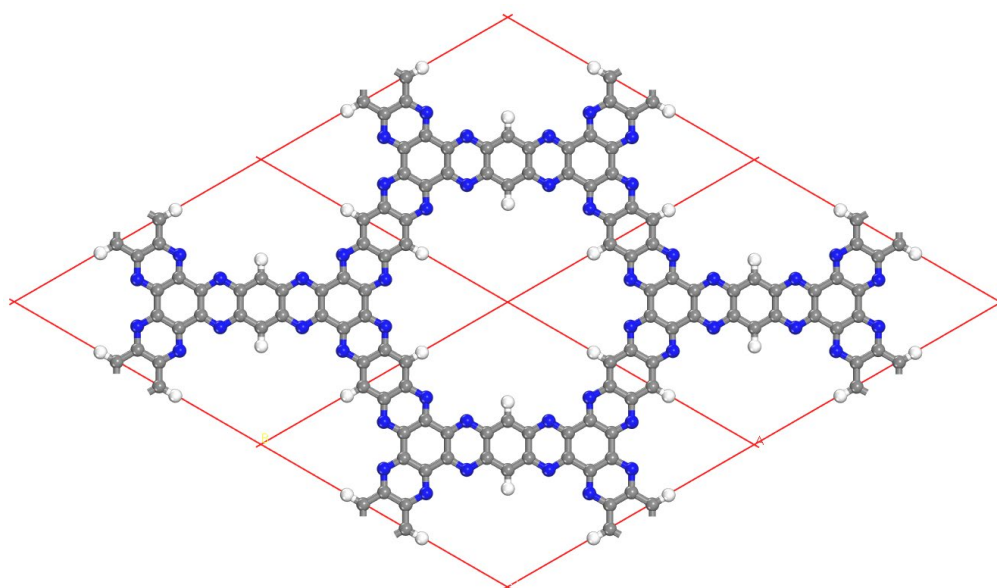


Figure S9. Supercell model of the **Aza-CMP**.

Figure S10.

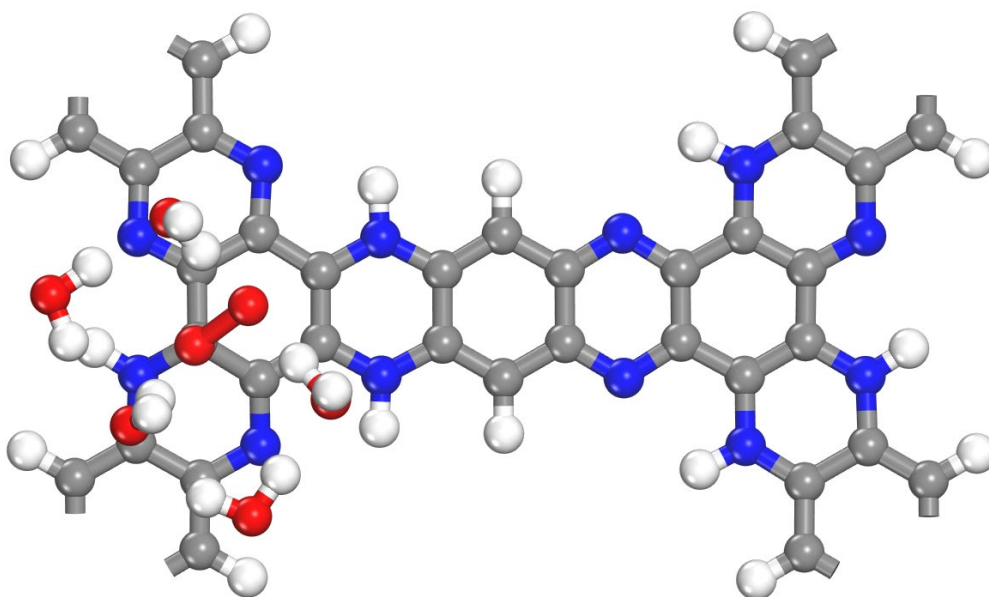


Figure S10. Adsorbent-adsorbate-solvent configuration corresponding to the fully optimized monodentate associative chemisorbed state of an oxygen molecule on top of the **Aza-CMP** estimated using five explicit water molecules in addition to the COSMO continuum model as solvation effect treatment.